

Original Research Article

Assessment of Vegetation Dynamics in a Semi-Arid Environment using Fuzzy Logic and Geospatial Approach: Evidence from Ngala Local Government Area, Borno State, Northeastern Nigeria

ABSTRACT

Semi-arid landscapes, particularly in conflict-affected regions such as northeastern Nigeria are exceptionally vulnerable to both climatic variability and anthropogenic disturbance, making the monitoring of vegetation dynamics crucial for ecological resilience and sustainable resource management. This study intends to integrate fuzzy logic with geospatial techniques to assess the vegetation dynamics in Ngala Local Government Area, from 2009-2024 and temporal intervals of five year were analyzed to capture spatiotemporal variations. Datasets from the Moderate Resolution Imaging Spectroradiometer (MODIS) and the Climate Hazards Group InfraRed Precipitation with Station data (CHIRPS) were processed in Google Earth Engine to analyze the nexus between vegetation dynamics and climatic parameters. The map visualization and layout were subsequently carried out in ArcGIS 10.8. Fuzzy Vegetation Risk Index (FVRI) and regression analysis were utilized to examine the vegetation vulnerability and ecological responses. Results of the study shown that rainfall increased from 527.07mm in 2009 to 692.85mm in 2019, before declining to 523.18mm in 2024, while LST decreased from 38.57°C to 35.27°C during the same period. Furthermore, NDVI yielded a similar trend, peaking at 0.351 in 2019 after declining to 0.324 in 2024. Regression results revealed a weak positive correlation between NDVI and rainfall ($R^2=0.254$) and a strong negative correlation with LST ($R^2=0.696$). FVRI analysis further revealed three vegetation phases, stability in 2009-2014 (82.8%), substantial improvement (99%) in 2014-2019 and a reversal toward 90% degradation during 2019-2024. This study ascertained that vegetation in semiarid environment is susceptible to climate fluctuations and human activities which highlighting the need for intervention to strengthen ecological resilience to support SDG 13 (Climate Action).

Keywords: Google Earth Engine, Fuzzy logic, NDVI, Semi-arid environment, Vegetation dynamics,

INTRODUCTION

Vegetation in semi-arid landscape plays a crucial role in regulating ecological, climatic, and anthropogenic interactions which significantly influence biodiversity, ecosystem services, and human livelihoods. The Semi-arid environments are characterized by irregular rainfall patterns, high evapotranspiration rates, and susceptible to environmental degradation as well as climate variability (Yan et al., 2022; Mukete et al., 2024). Globally, dryland environments account for over 41% of the Earth's land surface excluding North Atlantic region and providing sustenance for over 2 billion people across the region (Sardans et al., 2024; Dzvene et al., 2025).

Commented [J11]: yeras

Commented [J12]: was

In sub-Saharan Africa (SSA) region where drylands are predominated, vegetation dynamics are intensified and triggered by climatic variability and anthropogenic pressures (Hoscilo et al., 2015; Nzabarinda et al., 2021). Nigeria, the "giant of Africa" and one the most populous country in the region also reflects these challenges with its northern parts experiencing accelerated environmental pressures due to both natural and human stress like deforestation, overgrazing, land use and landcover changes and conflict related displacements (Okon et al., 2021; Abubakar et al., 2025). Borno State, which situated at the heart of the Lake Chad basin experienced a significant vegetation dynamic over the past decades, having a serious consequence for local communities that largely depend on Agricultural practices as major source of livelihood (Laminu, 2011). Thus, monitoring of vegetation dynamics in such regions is highly important for sustainable ecological management. However, the conventional vegetation monitoring often fails to capture the nature such complex semi-arid ecosystem (Shettima, et al 2025; Ingle et al., 2025), thereby necessitating the integration of fuzzy logic with geospatial techniques. By employing fuzzy and geospatial approach this study provides a more in-depth understanding of vegetation dynamic in the region.

The advancements in Geospatial technologies over the past decades have significantly enhanced the process of studying vegetation dynamics across spatiotemporal scale. In semi-arid environments, these technologies have become a novel approach for monitoring and assessing vegetation indices such as the Normalized Difference Vegetation Index (NDVI) and Enhanced Vegetation Index (EVI) which provide a quantitative measure for vegetation health and density (Uscanga, 2023; Zhao et al., 2024). Furthermore, geospatial modeling improved these assessments by integrating spatial data and climatic parameters into a predictive Approaches using machine learning algorithms (Singha, et al. 2024). Fuzzy logic has emerged as a powerful Model for handling the uncertainties inherent in environmental data which introduced by Lotfi A. Zadeh in 1965. It allows partial memberships, making it powerful mathematical tool for modeling vague concepts like healthy vegetation or degraded vegetation in dynamic ecosystems (Kumari, 2025). Recent applications include Evaluating land suitability for spatial planning in arid regions (Akbari et al., 2019), detection of desertification-prone areas (Shiravi & Sepehr, 2017), Smart soil health monitoring (Prasad et al., 2023) and Combination of fuzzy-AHP and GIS techniques in land suitability assessment for wheat cultivation. (Kilic et al., 2022). In the context of the African continent, several studies have employed fuzzy logic and GIS in semi-arid zones to study land suitability for surface irrigation (Haile & Abebe, 2022) and an irrigation improvement system for Nigerian agricultural fields (Ifeagwu & Okafor, 2024).

In spite of the novelty and advancements in fuzzy logic and geospatial approaches significant gaps persist in application to vegetation dynamics studies particularly in conflict affected regions like Borno State, Nigeria. Moreover, vegetation studies in Borno State largely employ only conventional GIS and remote sensing (Bukar et al., 2020; Bukar et al., 2024) without fuzzy model enhancements. Furthermore, few studies address the nexus between anthropogenic factors and natural drivers like climate variability. Therefore, this study bridges the gap by employ fuzzy logic-based framework for assessing vegetation dynamics in the semi-arid environment using Ngala LGA, Borno State, Nigeria as case study.

2. STUDY AREA AND METHODOLOGY

2.1. Study Area

Ngala Local Government Area (LGA) is located in Borno State, northeastern Nigeria and bordering Cameroon. It is located between latitude 12°0'0"N and 12°36'0"N and longitudes 14°0'0"E and 14°24'0"(Fig.1). Covering approximately 1, 342.8 km² with a population of over 237,000 at the 2006 census, primarily Kanuri and Hausa/Fulani speakers are the dominant, the area characterized by semi-arid climatic conditions, with significant seasonal variations in rainfall and temperature. The daily average temperatures are high throughout the year ranging between 25° C to 44° C whereas lower temperature is recorded in January and the highest in April. The rainy season lasts for about 60 days with annual rainfall of less than

Commented [J13]: approaches

Commented [J14]: update pls

Commented [J15]: put present before significant

700 mm (Laminu, 2011). It has elevation generally less than 320m above sea level (Fig. 1). The study area is dominated by flat plains of Lake Chad (Vertisols). These are heavy dark clay soils (locally called firgi or Firii), which develop wide cracks during the dry season (Shettima And Hassan, 2025). The Local government generally drained by seasonally receding River (Ebeji) whose peak flows are recorded during the month of November and December (Shettima and Hassan, 2025) and influenced by the Chad Basin's structural depression. Vegetation cover is predominantly savannah and cropland, which are sensitive to climatic variability and anthropogenic pressures. Agricultural practices are major socioeconomic activity in the LGA be it land cultivation, fishing or nomadism. It is a source of animal protein in this country being one of the producers of livestock and livestock products (Shettima and Hassan, 2025).

Commented [J16]: &

Commented [J17]: &

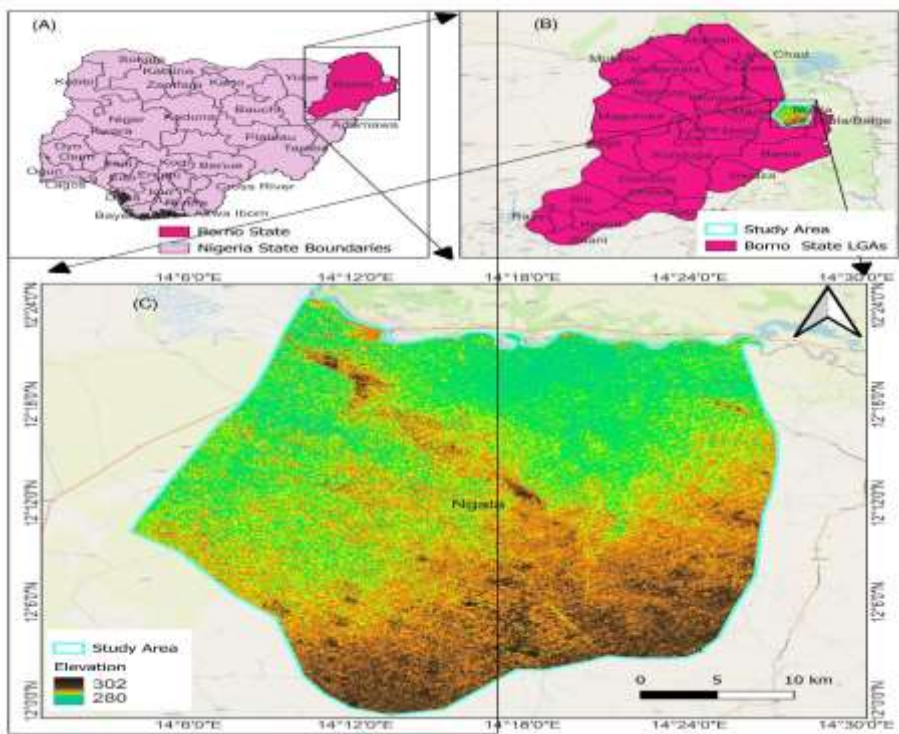


Fig 1: Description of the Study Area: (A) Nigeria showing Borno State, (B) Borno State Showing Ngala LGA, (C) Ngala Local Government Area (Study Area)

Source: Department of Environmental Science Integral University Lucknow and Author's work (2025)

2.2. Methodology

The three primary datasets utilized in this study include rainfall, land surface temperature (LST), and the Normalized Difference Vegetation Index (NDVI) for the years 2009, 2014, 2019, and 2024. For each study year, annual mean data were computed with five years interval (Fig..2). This temporal scope was adopted to ensure consistency across study years to avoid misleading trends (Tveito, 2023). All datasets were

accessed and processed through Google Earth Engine (GEE) (Table 1), cloud-based platform that developed by Google to address big data analysis challenges while also allowing the processing of huge amounts of remote sensing data over large areas and long-term environmental monitoring (Ghosh et al., 2022). All raster datasets were spatially constrained by clipping them to the administrative boundary of Ngala LGA. Temporal filtering was subsequently applied, whereby MODIS NDVI and LST collections were restricted to the designated study years (2009, 2014, 2019, and 2024), and CHIRPS rainfall data were aggregated into annual totals. Band selection and scaling procedures were also undertaken, with NDVI extracted from the MOD13Q1 product and adjusted using a scale factor of 0.0001, while MODIS LST measurements were converted from Kelvin to degrees Celsius using the recommended scale factor of 0.02. The framing, visualization, and map layout were subsequently carried out in ArcGIS 10.8.

Commented [J18]: remove

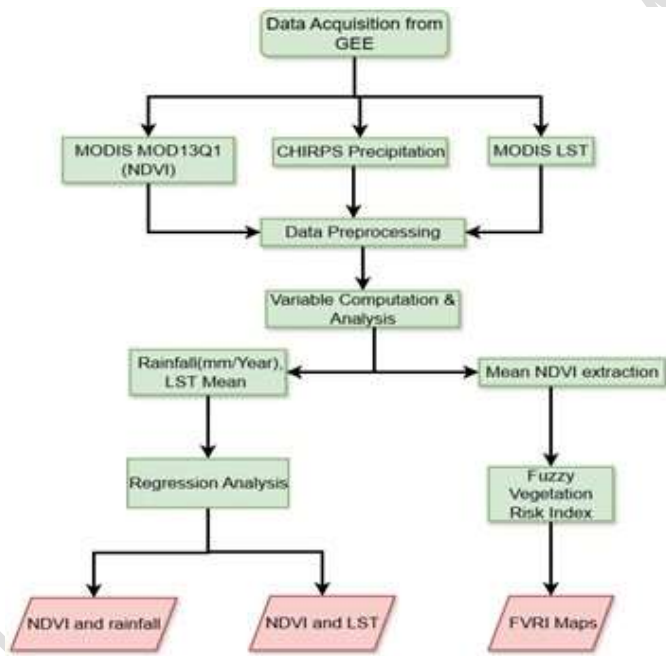


Fig.2: Methodological Flow chart

Table 1: The Source and Datasets used for the Study

Data Type	Dataset	Spatial Resolution	Links	Temporal Coverage	Purpose
-----------	---------	--------------------	-------	-------------------	---------

NDVI	MODIS MOD13Q1 NDVI V6.1	250 m		https://earthexplorer.usgs.gov/	2009–2024	Annual mean NDVI calculation for vegetation trend analysis
Precipitation (Rainfall)	CHIRPS	0.05° km)	(~5	https://www.chc.ucsb.edu/data/chirps	2009–2024	Annual rainfall accumulation for climate variability analysis
Land Surface Temperature (LST)	MODIS MOD11A1 LST V6.1	1 km		https://earthexplorer.usgs.gov/	2009–2024	Annual mean land surface temperature estimation
Administrative boundary	FAO(Global Administrative Unit Layers) Dataset	Vector		http://www.fao.org/geonetwork/srv/en/main.home	Static	Study area delineation (Ngala LGA)

2.2.1 Normalized Difference Vegetation Index (NDVI)

The Moderate Resolution Imaging Spectroradiometer (MODIS) MOD13Q1 Version 6.1 dataset was used to derive the Normalized Difference Vegetation Index (NDVI) at a 250m spatial resolution and a temporal resolution of 16 days (Anees et al., 2024). This dataset was widely used for change detection in vegetation health and growth, especially in semi-arid regions (Gholamnia et al. 2019). NDVI values range from -1 to +1, with values >0.4 indicating healthy vegetation and <0.2 signifying sparse or degraded cover (Afra, et al 2024; Bartold, et al 2024). NDVI was computed (equation 1).

$$NDVI = \frac{NIR-RED}{NIR+RED} \quad (Eq. 1)$$

Where: NIR = surface reflectance in the near-infrared band (841–876 nm) and RED= reflectance in the red band (620–670 nm). (Padawale et al., 2025; Nitu, et al 2025). For each year, the annual mean NDVI was computed (equation 2)

$$\bar{NDVI}_y = \frac{1}{n} \sum_{i=1}^n NDVI_i \quad (Eq. 2)$$

Where: n = number of 16-day composites in year y .

2.2.2 Vegetation Change Detection

NDVI change detection was performed for the periods 2009–2014, 2014–2019 and 2020–2024 which computed using equation 3.

$$\Delta NDVI = NDVI_{t,2} - NDVI_{t,1} \quad (Eq. 3)$$

NDVI Classification thresholds were applied. The vegetation cover maps are presented by thresholding NDVI values. The threshold values of the cover types were adopted from Mehta et al., (2021) (Table 2). These thresholds were derived from sensitivity analyses on NDVI variability in semi-arid regions.

Table 2: NDVI Value Threshold

Cover Type	NDVI Value Threshold	Description
------------	----------------------	-------------

Commented [J19]: remove

Commented [J110]: remove

Commented [J111]: remove Eq

Commented [J112]: remove

Commented [J113]: do same

Commented [J114]: remove

Commented [J115]: remove

Water	≤ -0.046	No vegetation presence
Bare Soil	≤ 0.25	No significant vegetation cover
Sparse Vegetation	≤ 0.35	Vegetation degradation
Moderate Vegetation	≤ 0.50	Stable vegetation cover
Dense Vegetation	≤ 1.00	Vegetation improvement

Source: Mehta et al., (2021)

2.2.3. Rainfall

The Climate Hazards Group InfraRed Precipitation with Station data (CHIRPS) dataset provided quasi-global daily rainfall estimates at 0.05° (~5 km) resolution from 1981 to near-present (Shen et al., 2020). CHIRPS blends satellite infrared observations with in-situ rain gauge measurements to produce reliable precipitation data with high-resolution and long-term records. (Ahana et al., 2024). Annual rainfall totals were derived from CHIRPS daily precipitation data by temporal aggregation using equation 4.

$$R_y = \frac{1}{n} \sum_{d=1}^n P_d \quad (\text{Eq. 4})$$

Where: R_y = total rainfall for year y ,

P_d = precipitation on day d ,

n = number of days in the year.

2.4 Land Surface Temperature (LST)

The MODIS MOD11A1 Version 6.1 dataset provides daily LST at 1 km resolution which retrieved from thermal infrared bands using the generalized split-window algorithm (TAN ET AL. 2021). LST serves as a proxy for thermal stress on vegetation, with higher values indicating potential drought conditions (CHOUDHURY, 2024) The annual mean LST for each year was computed (Equation 5).

$$\bar{LST}_y = \frac{1}{n} \sum_{i=1}^n LST_i \quad (\text{Eq. 5})$$

Where: LST_i = daily LST observation,

n = number of daily observations in year y .

2.5. Fuzzy Vegetation Risk Index (FVRI)

Fuzzy Vegetation Risk Index (FVRI) approach was utilized to vegetation vulnerability. This approach follows earlier applications of fuzzy modelling with NDVI for drought, Desertification, and vegetation risk assessment (Wang et al., 2015; Semeraro et al., 2019; Huang et al., 2023) which allows gradual classification of vegetation condition from degraded to healthy states rather than relying on binary output. It integrates NDVI change thresholds with fuzzy logic (Equation 6)

$$FVRI(x, y) = \begin{cases} 2, & \text{if } \Delta NDVI(x, y) > 0.05 \text{ (Improvement)} \\ 1, & \text{if } \Delta NDVI(x, y) < -0.05 \text{ (Degradation)} \\ 0, & \text{if } -0.05 \leq \Delta NDVI(x, y) \leq 0.05 \text{ (No Change)} \end{cases}$$

where: $\Delta NDVI(x, y) = NDVI_{t_2}(x, y) - NDVI_{t_1}(x, y)$ (Eq. 6)

Commented [J116]: remove

Commented [J117]: remove

Commented [J118]: capital letter?

Commented [J119]: remove and move to literature

Commented [J120]: remove

Commented [J121]: move to literature

Commented [J122]: remove

x, y = pixel coordinates in between two time periods t_1 and t_2 .

The thresholds ± 0.05 are used to determine significant changes in vegetation condition. Vegetation classes (improved, degraded, stable) were converted into areas in hectares (equation 7) and percentages using pixel area (equation 8). The spatial extent of each FVRI class and fuzzy membership was computed in hectares:

$$A_c = \sum_i^{N_c} \text{PixelArea}_i \quad (\text{Eq. 7})$$

$$\%A_c = \frac{A_c}{A_{\text{total}}} \times 100 \quad (\text{Eq. 8})$$

where N_c = number of pixels in class c , and A_{total} = total LGA area.

2.6. Regression Analysis

Relationship between NDVI and rainfall: Vegetation health is strongly influenced by rainfall availability. A simple linear response model (equation 9).

$$\text{NDVI} = \alpha \cdot P + \varepsilon \quad (\text{Eq. 9})$$

Where: NDVI = vegetation greenness index

P = rainfall (mm/year, from CHIRPS)

α = sensitivity coefficient (how strongly NDVI responds to rainfall)

ε = residual term accounting for other environmental factors

Relationship between NDVI and LST: A simple regression can describe the dependence of NDVI on LST (equation 10).

$$\text{NDVI} = \beta \cdot \text{LST} + \varepsilon \quad (\text{Eq. 10})$$

Where: NDVI = Normalized Difference Vegetation Index

LST = Land Surface Temperature ($^{\circ}\text{C}$, derived from MODIS or Landsat thermal bands)

β = regression coefficient indicating the rate of NDVI change per unit increase in temperature

ε = residual term (unexplained variance due to soil, rainfall, human activity, etc.)

Scatter plots with fitted regression lines were generated to visualize direct (NDVI-Rainfall) and inverse (NDVI-LST) associations.

3. RESULT AND DISCUSSION

3.1. Spatiotemporal Variation Among Rainfall, Land Surface Temperature (LST), and NDVI

Vegetation greenness in the semi-arid environments is closely related to seasonal rainfall and LST distribution over different ecological zones (Ayanlade et al., 2021; Zeng et al., 2023). Seasonal rainfall and LST distribution are critical factors influence vegetation dynamics in this semi-arid Sahelian environment

Commented [J123]: do same

Commented [J124]: do same

Commented [J125]: was

Commented [J126]: do same

Commented [J127]:

Commented [J128]: could

Commented [J129]: remove

(Li et al., 2025). Fig. 3 shows the annual mean rainfall, land surface temperature (LST) and NDVI in Ngala LGA from 2009 to 2024.

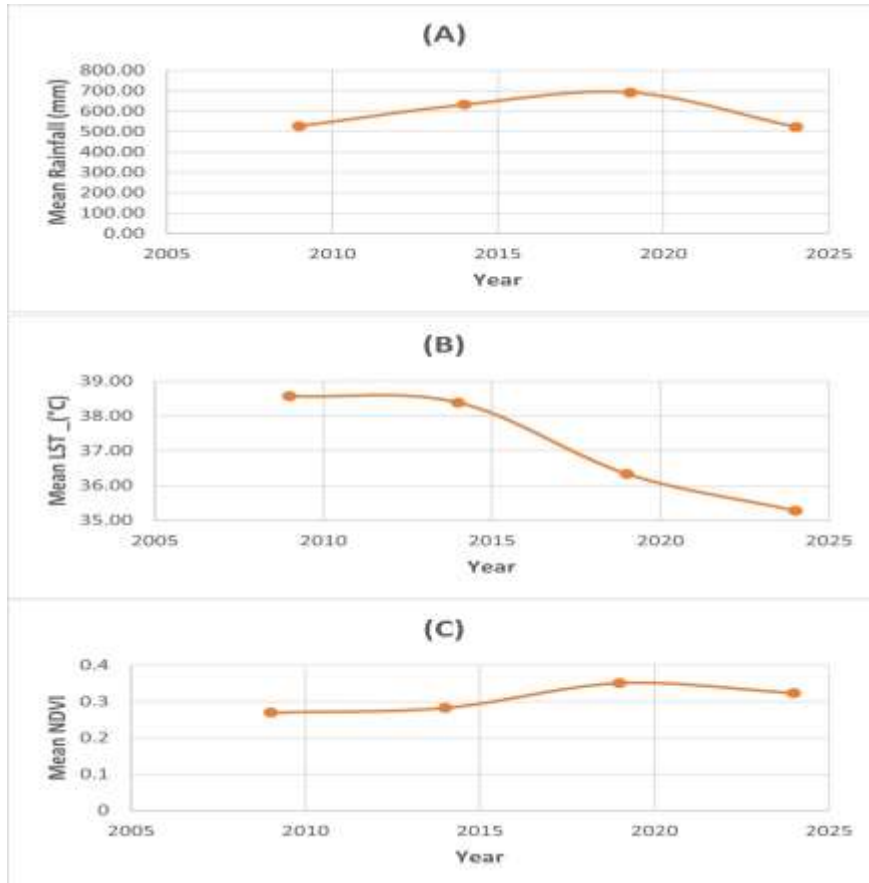


Fig. 3: Annual mean variations of: (A) Rainfall, (B) Land Surface Temperature variation, (C) NDVI trend for Ngala LGA (2009–2024).

Rainfall pattern shown an increasing from 527.07 mm in 2009 to 692.85 mm in 2019 and subsequently declining to 523.18 mm in 2024 (Fig. 3(A)). LST shown a steady decreasing from 38.57 °C in 2009 to 35.27 °C in 2024 (Fig. 3(B)). However, the NDVI yielded rising trend from 0.27 in 2009 to a peak of 0.351 in 2019 before slightly decline to 0.324 in 2024 (Fig. 3(C)). These results indicate strong positive correlation between rainfall and NDVI implying that increased precipitation improves vegetation greenness. Contrarily, an inverse relationship was observed between LST and NDVI, indicating that higher land surface temperatures are associated with vegetation degradation. This finding corroborate study conducted in semi-arid Basin of Western China By Li et al., (2025) where Vegetation indices are positively correlated with

precipitation and high temperatures leading to a decline in greenness and a negative correlation between LST and NDVI.

3.2. Mean NDVI Change Trend (2009–2024).

The mean NDVI change trend between 2009 and 2024 indicates a dynamic trajectory in vegetation greenness, reflecting both periods of improvement and degradation (Fig. 4). Such fluctuations indicates that vegetation cover in semi-arid environments is influenced by multiple drivers including Climate variability and anthropogenic activities (Deng et al., 2022). Fig. 5 summarizes the variation of vegetation cover between 2009-2014, 2014-2019, and 2019-2024 in Ngala LGA, from strongest greening occurred during 2014-2019 (+0.289) to stronger negative shifts (-0.186) during 2019-2024, reflecting vegetation degradation in parts of the LGA.

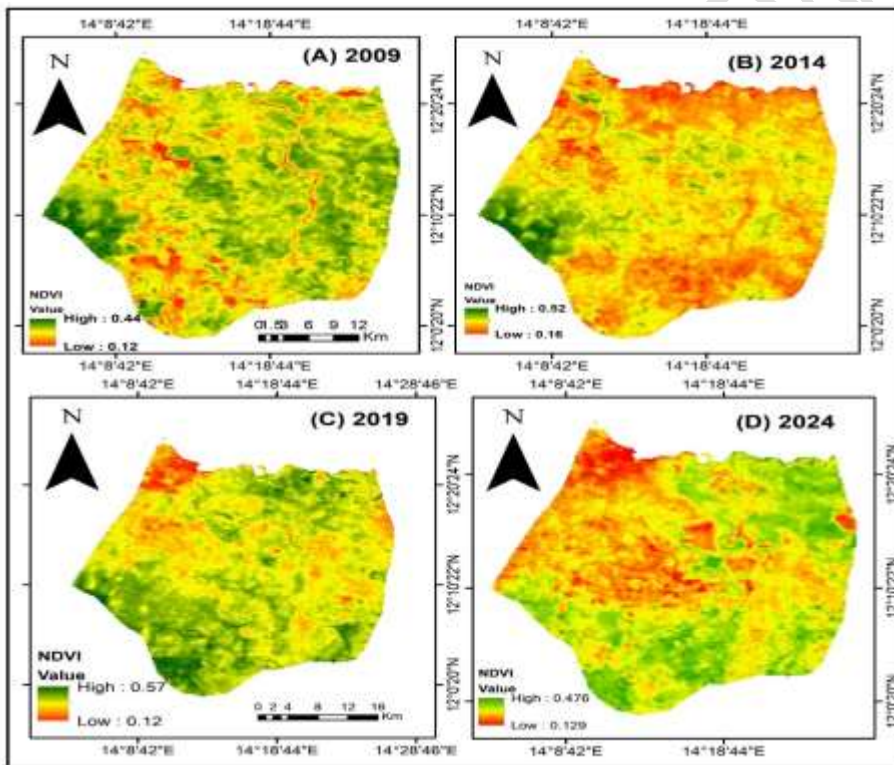


Fig. 4: Mean NDVI Maps of Ngala LGA for: (A) 2009, (B) 2014, (C) 2019, (D) 2024

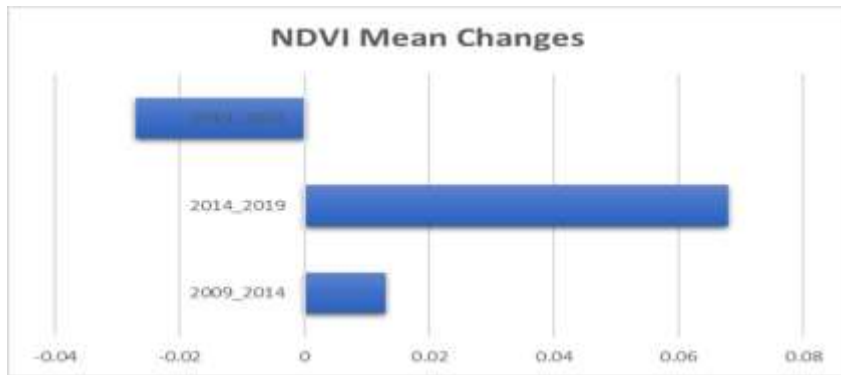


Fig. 5: Mean NDVI change rates (2009–2024).

The increase in NDVI between 2014 and 2019 (Fig. 5) indicates favorable climatic conditions relatively associated with years rainfall above the average. Similar patterns have been observed in the semi-arid region, where vegetation indices typically rise following wet years and decline during droughts (Rousta, et al. 2020). conversely, the decline between 2019 and 2024 demonstrates irregular rainfall patterns which reduce greenness(Fig.5). These findings are consistent with broader Sahel studies that emphasize the sensitivity of vegetation cover to short-term climate variability (Lu et al., 2024; Ahmed, et al 2024)

Commented [J130]: emphasized

Anthropogenic factor also plays a significant role in vegetation cover dynamics (Feng et al., 2020). In the study area, Livelihoods heavily depend on rainfed Farming, livestock grazing, and fuelwood collection like many other semi-arid regions. The gradual improvement in vegetation greenness up to 2019(Fig.5) may be attributed to reduction of human activity in insecure rural area as result of Insurgency which allowed for short-term vegetation regeneration. This finding is consistent with study conducted in the region by Shettima et al., (2025), where vegetation gains prior to the peak insurgency years were gradual, while a sharp increase during peak insurgency resulted from reduction of anthropogenic disturbance. However, as displaced populations resettled in concentrated safe zones, the demand for land and fuelwood increased, contributing to localized vegetation degradation during 2019-2024(Fig.5). Therefore, the impact of conflict on climate variability functioned both direct and indirect, depending on the changes in non-climate variables such as water security, yield, and income. (Xie et al., 2022).

Commented [J131]: remove

3.3. Regression Analysis between NDVI, Rainfall, and LST

The regression analysis between NDVI, rainfall, and LST reveals important ecological insights into vegetation dynamics between 2009 and 2024 (Fig. 6). NDVI and climatic variables relationship across different vegetation types is critical to predicting the vegetation dynamics and effective ecological restoration management (Gao, et al 2022; Mehmood, et al. 2024)

Commented [J132]: is this your result or literature? remove

3.3.1. Rainfall vs NDVI and LST vs NDVI

The regression equation obtained was: $NDVI = 0.173 + 0.000226 \cdot Rainfall, R^2 = 0.254$ (Fig. 5A) This indicates a positive but weak relationship between rainfall and NDVI. The result demonstrate that higher rainfall generally supports an increase in vegetation greenness however, the relatively low coefficient of determination ($R^2 = 0.254$) implies that rainfall alone explains only about 25.4% of the variation in NDVI and Other factors such as anthropogenic pressure plays a significant role in determining vegetation health.

Relevant studies in semi-arid region suggest also a weak positive correlation between vegetation NDVI and interannual precipitation (Lu et al., 2025) which is consistent with the findings of this study.

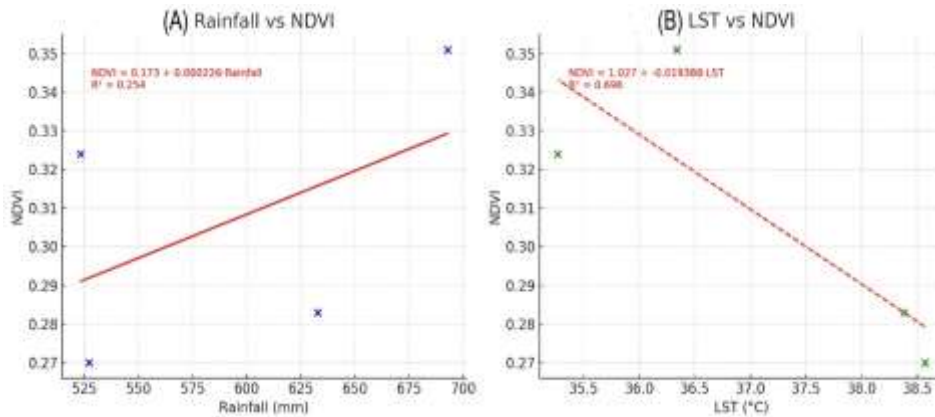


Fig.6: Regression analysis between: (A) NDVI and Rainfall, (B) NDVI and LST

The regression equation obtained was: $NDVI = 1.027 - 0.019388 \cdot LST$, $R^2 = 0.696$ (Fig.6B). This reveals a strong negative relationship between LST and NDVI. As land surface temperature increases, NDVI decreases significantly indicating that vegetation greenness is highly sensitive to LST With an $R^2 = 0.696$, approximately 69.6% of the variation in NDVI. A study carried out in Thailand reported also negative correlation between LST and NDVI and various factors, including seasonal variations, spatial heterogeneity, and anthropogenic activities influenced the relationship (Kliengchuay et al., 2025). This finding is ecologically consistent as the high temperatures increase evapotranspiration rates and soil moisture depletion which coincide with drought conditions and land degradation processes, particularly in semi-arid ecosystems (Olagunju, 2015; Dai, et al 2022)

3.4. Fuzzy Vegetation Risk Index (FVRI)

The FVRI for Ngala LGA across the three periods (2009-2014, 2014-2019, and 2019-2024) yields important spatiotemporal transitions in vegetation condition (Fig.7). For 2009-2014 period (Fig. 7A), the FVRI values clustered between -0.0499 and -0.0018 (Degraded) -0.0018 and 0.0304 (Stable), and >0.0304 (improvement), indicating a mosaic landscape where localized degradation coexisted with broad areas of stability and resilience. By 2014-2019, the classification ranges from -0.0494 to 0.0390 and >0.0390 (Fig. 7B) where vegetation improvement was observed in the majority of the areas indicating optimal vegetation conditions across most of the study area. Nevertheless, during 2019-2024, the FVRI classes ranges from -0.0499 to -0.0178 , -0.0178 to 1.0031 and >1.0031 (Figure 16) revealed a marked expansion of degraded areas, with very few areas exceeding the healthy threshold, confirming the severe decline detected in the aggregated statistics ~90% degradation (Fig. 7C). This progression shows a temporal trajectory from mixed conditions (2009-2014), to widespread improvement (2014-2019) and finally to severe degradation (2019-2024). Such dynamics are consistent with Vegetation responses in the semi-arid environment where significant greening following wet years, but this recovery is often fragile subsequent droughts, heat stress, and anthropogenic pressures can rapidly reverse gains in vegetation cover and productivity (Vicente-Serrano et al., 2013; Verbruggen et al., 2021). (Fig. 8) shows Vegetation changes (area in hectares) in Ngala LGA,

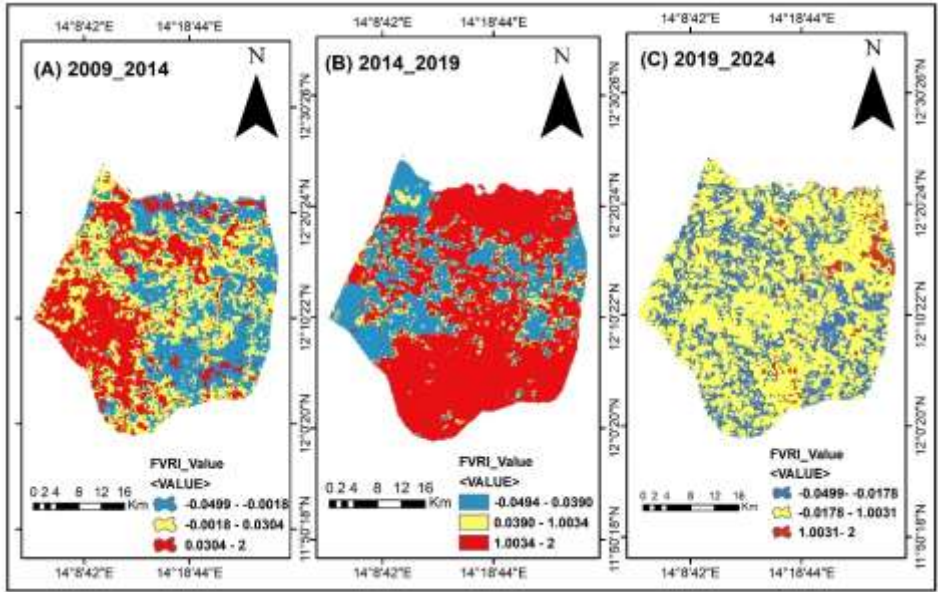


Fig. 7: FVRI for Ngala LGA from: (A) 2009-2014, (B) 2014-2019 (C) 2019-2024

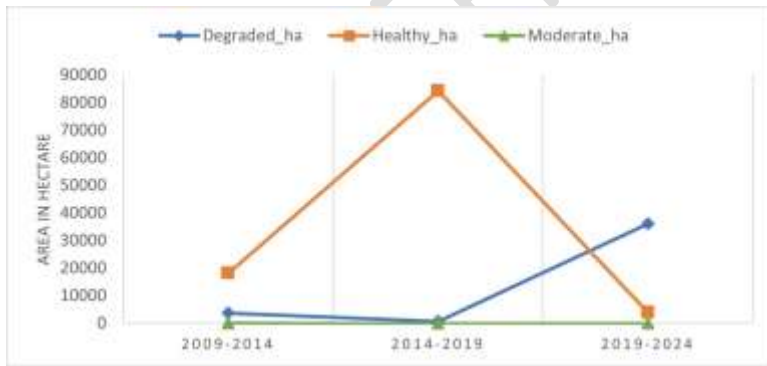


Fig. 8: Vegetation Changes Area (Hectares) over the Study Period in Ngala LGA

The result demonstrates a clear temporal shift in vegetation across the study periods. Between 2009 and 2014, vegetation remained largely stable, with approximately 82.8% (18,151 ha) of the land classified as healthy (Fig. 8) and 17.2% (3,741 ha) experiencing degradation. A significant improvement occurred during 2014-2019 (Fig. 8) when vegetation health peaked at over 99% (84,336 ha), indicating favorable climatic conditions and reduced stressors. However, this trend was drastically reversed in the subsequent period (2009-2024), with nearly 90% (36,099 ha) of vegetation degraded and less than 10% (3,927 ha) remaining healthy (Fig. 8). These findings are consistent with several reports on declining in semi-arid vegetation

resilience as a result of increasing climatic variability and human illegal activities significantly reduced (Kiribou et al. 2025).

4. CONCLUSION AND RECOMMENDATION

This study highlighted a strong sensitivity of vegetation cover to both climatic variability and anthropogenic pressure in a semi-arid landscape. Rainfall reflects positive but weak influence on the vegetation greenness, simultaneously land surface temperature reflects a strong negative relationship with vegetation, indicating the vulnerability of semi-arid ecosystems to rising temperatures. Furthermore, findings on temporal trends demonstrated a significant greening between 2014 and 2019, followed by widespread degradation after 2019, depicting a combined effect of climatic variation, rising human pressures and Conflict related land-use changes. The Fuzzy Vegetation Risk Index further affirmed that vegetation health peaking at over 99% in 2019 before drastically declining to nearly 90% degradation by 2024. These findings emphasize the vulnerability of semi-arid ecosystems and the critical need for climate resilient vegetation management strategies such as afforestation, rangeland restoration, and sustainable agriculture to support the Sustainable Development goals (SDG 13) Climate Action and (SDG 15) Life on Land. Moreover, this study indicate that Fuzzy logic and geospatial techniques Integration can not only enables real time monitoring of vegetation but also handling the uncertainties inherent in spatial data and climatic parameters.

REFERENCES

1. Abubakar, A. S., Bello, N. I., & Ismail, A. H. (2025). Navigating environmental migration in Nigeria: Trends, impacts, and strategic responses. *International Journal of Environmental Pollution and Environmental Modelling*, 8(1), 1-10. <https://dergipark.org.tr/en/download/article-file/3900000>
2. Afra, I. L. F., Iyob, A. L., & Nuskiya, M. H. F. (2024). Change detection of vegetation cover using NDVI: A case of Harispattuwa Divisional Secretariat Division in Kandy District. *Colombo Geographer*, 2,2: 71–87.
3. Ahana, B. S., Posite, V. R., Maouly, D. K., Cherifa, A., Kantoush, S. A., Nguyen, B. Q., & Kumar, N. (2024). Changing Rainfall Patterns in the Northeastern South Kivu Region, Democratic Republic of the Congo: A Detailed Analysis Using CHIRPS Rainfall Data (1981–2023). *Earth Systems and Environment*. <https://doi.org/10.1007/s41748-024-00510-0>
4. Ahmed, S. M., Dinnar, H. A., Ahmed, A. E., Elbushra, A. A., & Turk, K. G. B. (2024). A Deeper Understanding of Climate Variability Improves Mitigation Efforts, Climate Services, Food Security, and Development Initiatives in Sub-Saharan Africa. *Climate*, 12(12), 206. <https://doi.org/10.3390/cli12120206>
5. Akbari, M., Neamatollahi, E., & Neamatollahi, P. (2019). Evaluating land suitability for spatial planning in arid regions of eastern Iran using fuzzy logic and multi-criteria analysis. *Ecological Indicators*, 98, 587–598. <https://doi.org/10.1016/j.ecolind.2018.11.035>
6. Anees, S. A., Mehmood, K., Rehman, A., Rehman, N. U., Muhammad, S., Shahzad, F., Hussain, K., Luo, M., Alarfaj, A. A., Alharbi, S. A., & Khan, W. R. (2024). Unveiling fractional vegetation cover dynamics: A spatiotemporal analysis using MODIS NDVI and machine learning. *Environmental and Sustainability Indicators*, 24, 100485. <https://doi.org/10.1016/j.indic.2024.100485>
7. Ayanlade, A., Jeje, O. D., Nwaezeigwe, J. O., Orimoogunje, O. O. I., & Olokeogun, O. S. (2021). Rainfall seasonality effects on vegetation greenness in different ecological zones. *Environmental Challenges*, 4, 100144. <https://doi.org/10.1016/j.envc.2021.100144>
8. Bartold, M., Wróblewski, K., Kluczek, M., Dąbrowska-Zielińska, K., & Goliński, P. (2024). Examining the Sensitivity of Satellite-Derived Vegetation Indices to Plant Drought Stress in Grasslands in Poland. *Plants*, 13(16), 2319. <https://doi.org/10.3390/plants13162319>
9. Bukar, M. A., Bukar, W. M., Bakari, K., & Mbaya, R. P. (2020). Monitoring vegetation change using NDVI analysis and image differencing from Landsat imagery in North-Eastern Nigeria, 1975-2016.

- IOSR Journal of Environmental Science, Toxicology and Food Technology, 14(10), 26–34. <https://doi.org/10.9790/2402-1410032634>
10. Bukar, W. M., Umar, I. A., & Jimme, M. A. (2024). Seasonal variability of normalized difference vegetation index (NDVI) and the influence of internally displaced persons (IDPs) in Maiduguri and environs, Northeast Nigeria. *International Journal of Novel Research and Development*, 9(7), e303-e316. <https://ijnrd.org/papers/IJNRD2407396.pdf>
 11. Choudhury, A. (2024). Drought trend and its association with land surface temperature (LST) over homogeneous drought regions of India (2001–2019). *Discover Water*, 4: 51. <https://doi.org/10.1007/s43832-024-00115-8>
 12. Dai, X., Yu, Z., Matheny, A. M., Zhou, W., & Xia, J. (2022). Increasing evapotranspiration decouples the positive correlation between vegetation cover and warming in the Tibetan plateau. *Frontiers in Plant Science*. <https://doi.org/10.3389/fpls.2022.974745>
 13. Deng, G., Gao, J., Jiang, H., Li, D., Wang, X., Wen, Y., Sheng, L., & He, C. (2022). Response of vegetation variation to climate change and human activities in semi-arid swamps. *Frontiers in Plant Science*. <https://doi.org/10.3389/fpls.2022.990592>
 14. Dzvene, A. R., Zhou, L., Slayi, M., & Dirwai, T. L. (2025). A scoping review on challenges and measures for climate change in arid and semi-arid agri-food systems. *Discover Sustainability* <https://doi.org/10.1007/s43621-025-00945-z>
 15. Feng, D., Yang, C., Fu, M., Wang, J., Zhang, M., Sun, Y., & Bao, W. (2020). Do anthropogenic factors affect the improvement of vegetation cover in resource-based region. *Journal of Cleaner Production* <https://doi.org/10.1016/j.jclepro.2020.122705>
 16. Gao, W., Zheng, C., Liu, X., Lu, Y., Chen, Y., Wei, Y., & Ma, Y. (2022). NDVI-based vegetation dynamics and their responses to climate change and human activities from 1982 to 2020: A case study in the Mu Us Sandy Land, China. *Ecological Indicators*, 137, 108745. <https://doi.org/10.1016/j.ecolind.2022.108745>
 17. Gholamnia, M., Khandan, R., Bonafoni, S., & Sadeghi, A. (2019). Spatiotemporal analysis of MODIS NDVI in the semi-arid region of Kurdistan (Iran). *Remote Sensing*, 11(14), 1723. <https://doi.org/10.3390/rs11141723>
 18. Ghosh, S., Kumar, D., & Kumari, R. (2022). Cloud-based large-scale data retrieval, mapping, and analysis for land monitoring applications with Google Earth Engine (GEE). *Environmental Challenges*, 9, 100605. <https://doi.org/10.1016/j.envc.2022.100605>
 19. Haile, M. M., & Abebe, A. K. (2022). GIS and fuzzy logic integration in land suitability assessment for surface irrigation: The case of Guder watershed, Upper Blue Nile Basin, Ethiopia. *Applied Water Science* <https://doi.org/10.1007/s13201-022-01761-w>
 20. Hoscilo, A., Balzter, H., Bartholomé, E., Boschetti, M., Brivio, P. A., Brink, A., Clerici, M., & Pekel, J. F. (2015). A conceptual model for assessing rainfall and vegetation trends in sub-Saharan Africa from satellite data. *International Journal of Climatology*, 35(13), 3582-3592. <https://doi.org/10.1002/joc.4231>
 21. Huang, B., Zha, R., Chen, S., Zha, X., & Jiang, X. (2023). Fuzzy evaluation of ecological vulnerability based on the SRP-SES method and analysis of multiple decision-making attitudes based on OWA operators: A case of Fujian Province, China. *Ecological Indicators*. <https://doi.org/10.1016/j.ecolind.2023.110432>
 22. Ifeagwu, E. N., & Okafor, J. O. (2024). Fuzzy-based irrigation improvement system for Nigerian agricultural fields. *Caritas Journal of Engineering Technology* <https://www.caritasuniversityjournals.org/index.php/cjet/article/view/100>
 23. Ingle, S. N., Mondal, B. P., Patel, C., & Prasad, J. (2025). Leveraging remote sensing and geospatial technologies in soil and water resources mapping and characterization: A review. *Agricultural Reviews*, 46(5), 703-711. <https://doi.org/10.18805/ag.r-2789>

24. Kilic, O. M., Ersayın, K., Gunal, H., Khalofah, A., & Alsubeie, M. S. (2022). Combination of fuzzy-AHP and GIS techniques in land suitability assessment for wheat (*Triticum aestivum*) cultivation. *Saudi Journal of Biological Sciences*, 29(4), 2634-2644. <https://doi.org/10.1016/j.sjbs.2021.12.050>
25. Kiribou, I. A. R., Nikiema, T., Dimobe, K., Zoungrana, B. J.-B., Ouedraogo, V., Yang, H., Santika, T., & Dejene, S. W. (2025). Climate change and variability as drivers of vegetation dynamics in Bontoli Natural Reserve, West African drylands. *Environmental Challenges*, 20, 101175. <https://doi.org/10.1016/j.envc.2025.101175>
26. Kliengchuay, W., Phonphan, W., Niampradit, S., Kiangkoo, N., Srimanus, W., Niemmanee, T., Arunplod, C., Wen, B., Guo, Y., Herbreteau, V., & Tantrakarnapa, K. (2025). Variation of vegetation cover and the relationship with land surface temperature across Thailand (2007 to 2022). *Scientific Reports*, 15, 27823. <https://doi.org/10.1038/s41598-025-13018-y>
27. Kumari, K. (2025). Fuzzy sets and fuzzy logic: A review of concepts, trends, and applications. *International Journal of Physics and Mathematics*. <https://doi.org/10.33545/26648636.2025.v7.i2b.140>
28. Lamini, S. (2011). 'Assessment Socioeconomic activities on lake chad floor area of Wulgo District, Ngala Local government area, borno state'. *An Unpublished M.Sc. Dissertation submitted to Department of Geography, University of Maiduguri*.
29. Li, L., Xia, R., Dou, M., Ling, M., Li, G., Wang, C., & Mi, Q. (2025). Integrating Landsat NDVI data with climate and anthropogenic factors reveals drivers of vegetation dynamics in the semi-arid Basin of Western China. *Scientific Reports*, 15, 18831. <https://doi.org/10.1038/s41598-025-02360-w>
30. Lu, T., Zhang, W., Abel, C., Horion, S., Brandt, M., Huang, K., & Fensholt, R. (2024). Changes in vegetation-water response in the Sahel-Sudan during recent decades. *Journal of Hydrology: Regional Studies*, 52, 101672. <https://doi.org/10.1016/j.ejrh.2024.101672>
31. Lu, Y., Yu, Y., Sun, L., Li, C., He, J., Guo, Z., Duan, L., Zhang, J., & Yu, R. (2025). NDVI based vegetation dynamics and responses to climate change and human activities at Xinjiang from 2001 to 2020. *Scientific Reports*. <https://doi.org/10.1038/s41598-025-11677-5>
32. Mehmood, K., Anees, S. A., Muhammad, S., Hussain, K., Shahzad, F., Liu, Q., Ansari, M. J., Alharbi, S. A., & Khan, W. R. (2024). Analyzing vegetation health dynamics across seasons and regions through NDVI and climatic variables. *Scientific Reports* <https://doi.org/10.1038/s41598-024-62464-7>
33. Mukete, B., Lori, T., Mukete, T., & Mukete, N. (2024). Analysis of the impacts of climate variations across semi-arid and arid regions of Southeast Africa. *Asian Scientific Bulletin*, 2(1), 105-111. <https://doi.org/10.17311/asb.2024.105.111>
34. Mehta, A., Shukla, S., & Rakholia, S. (2021). Vegetation change analysis using normalized difference vegetation index and land surface temperature in Greater Gir Landscape. *Journal of Scientific Research*, 65(3), 1-6. <https://doi.org/10.37398/JSR.2021.650301>
35. Nițu, A., Florea, C., Ivanovici, M., & Racovițeanu, A. (2024). NDVI and Beyond: Vegetation Indices as Features for Crop Recognition and Segmentation in Hyperspectral Data. *Sensors*, 24(12), 3817. <https://doi.org/10.3390/s24123817>
36. Nzabarinda, V., Bao, A., Xu, W., Uwamahoro, S., Jiang, L., Duan, Y., Nahayo, L., Yu, T., Wang, T., & Long, G. (2021). Assessment and evaluation of the response of vegetation dynamics to climate variability in Africa. *Sustainability* <https://doi.org/10.3390/su13031234>
37. Okon, E. M., Falana, B. M., Solaja, S. O., Yakubu, S. O., Alabi, O. O., Okikiola, B. T., Awe, T. E., Adesina, B. T., Tokula, B. E., Kipchumba, A. K., & Edeme, A. B. (2021). Systematic review of climate change impact research in Nigeria: Implication for sustainable development. *Heliyon*, 7(9), e07941. <https://doi.org/10.1016/j.heliyon.2021.e07941>

38. Olagunju, T. E. (2015). Drought, desertification and the Nigerian environment: A review. *Journal of Ecology and the Natural Environment*. <https://doi.org/10.5897/JENE2015.0523>
39. Padawale, A. P., Patake, P. R., Attar, A., & Kothiwale, R. A. (2025). NDVI Analysis And Visualization Using Sentinel Hub And Streamlit. *International Journal of Creative Research Thoughts (IJCRT)*, 13(5), 350-359. <https://www.ijcrt.org/papers/IJCRT2505733.pdf>
40. Prasad, R., Tiwari, R., & Srivastava, A. K. (2023). Internet of Things-Based Fuzzy Logic Controller for Smart Soil Health Monitoring: A Case Study of Semi-Arid Regions of India. *Engineering Proceedings* <https://doi.org/10.3390/ecsa-10-16208>
41. Rousta, I., Olafsson, H., Moniruzzaman, M., Zhang, H., Liou, Y.-A., Mushore, T. D., & Gupta, A. (2020). Impacts of Drought on Vegetation Assessed by Vegetation Indices and Meteorological Factors in Afghanistan. *Remote Sensing*, 12(15), 2433. <https://doi.org/10.3390/rs12152433>
42. Sardans, J., Miralles, A., Tariq, A., Zeng, F., Wang, R., & Peñuelas, J. (2024). Growing aridity poses threats to global land surface. *Communications Earth & Environment*. <https://doi.org/10.1038/s43247-024-01935-1>
43. Semeraro, T., Mastroleo, G., Pomes, A., Luvisi, A., Gissi, E., & Aretano, R. (2019). Modelling fuzzy combination of remote sensing vegetation index for durum wheat crop analysis. *Computers and Electronics in Agriculture*, 156, 684-692. <https://doi.org/10.1016/j.compag.2018.12.027>
44. Shen, Z., Yong, B., Gourley, J. J., Qi, W., Lu, D., Liu, J., Ren, L., Hong, Y., & Zhang, J. (2020). Recent global performance of the Climate Hazards group Infrared Precipitation (CHIRP) with Stations (CHIRPS). *Journal of Hydrology*, 591, 125284. <https://doi.org/10.1016/j.jhydrol.2020.125284>
45. Shettima, M., & Hassan, G. S. (2025). A geo-spatial approach to assess the distribution and accessibility of healthcare facilities in Ngala Local Government Area, Borno State. *Irish Journal of Environment and Earth Sciences*, 9(1), 109-118. <https://aspjournals.org/Journals/index.php/ijeas/article/view/573>
46. Shettima, M., Hasnat, M., Sambo, G. H., Bukar, A. G., Boyoma, A. M., & Mohammed, M. A. (2025). Spatio-Temporal Dynamics and Forecasting of Urban Land Use and Land Cover Change in Maiduguri Using Google Earth Engine and Machine Learning. *Arid Zone Journal of Engineering, Technology and Environment*, 21(3), 783-793. <https://www.azojete.com.ng/index.php/azojete/article/view/1121>
47. Shiravi, M., & Sepehr, A. (2017). Fuzzy based detection of desertification-prone areas: A case study in Khorasan-Razavi Province, Iran. *Natural Resources and Conservation*. <https://doi.org/10.13189/nrc.2017.050101>
48. Singha, C., Rana, V. K., Pham, Q. B., Nguyen, D. C., & Łupikasza, E. (2024). Integrating machine learning and geospatial data analysis for comprehensive flood hazard assessment. *Environmental Science and Pollution Research International*, 31(35), 48497-48522. <https://doi.org/10.1007/s11356-024-34286-7>
49. Tan, J., Che, T., Wang, J., Liang, J., Zhang, Y., & Ren, Z. (2021). Reconstruction of the Daily MODIS Land Surface Temperature Product Using the Two-Step Improved Similar Pixels Method. *Remote Sensing*, 13(9), 1671. <https://doi.org/10.3390/rs13091671>
50. Tveito, O. E. (2023). The effect of homogenization when constructing long-term gridded monthly precipitation and temperature data. *International Journal of Climatology*. <https://doi.org/10.1002/joc.8283>
51. Uscanga, A. (2023). Tracking vegetation changes with time series of satellite images. *Nature Reviews Earth & Environment*, 4(8), 513. <https://doi.org/10.1038/s43017-023-00444-7>
52. Verbruggen, W., Schurgers, G., Horion, S., Ardö, J., Bernardino, P. N., Cappelaere, B., Demarty, J., Fensholt, R., Kergoat, L., Sibret, T., Tagesson, T., & Verbeeck, H. (2021). Contrasting responses

- of woody and herbaceous vegetation to altered rainfall characteristics in the Sahel. *Biogeosciences*, 18(1), 77–93. <https://doi.org/10.5194/bg-18-77-2021>
53. Vicente-Serrano, S. M., Gouveia, C., Camarero, J. J., Beguería, S., Trigo, R., López-Moreno, J. I., Azorín-Molina, C., Pasho, E., Lorenzo-Lacruz, J., Revuelto, J., Morán-Tejeda, E., & Sanchez-Lorenzo, A. (2013). Response of vegetation to drought time-scales across global land biomes. *Proceedings of the National Academy of Sciences of the United States of America*, 110(1), 52–57. <https://doi.org/10.1073/pnas.1207068110>
54. Wang, Y., Zhang, J., Guo, E., & Sun, Z. (2015). Fuzzy comprehensive evaluation-based disaster risk assessment of desertification in Horqin Sand Land, China. *International Journal of Environmental Research and Public Health*, 12(2), 1703–1725. <https://doi.org/10.3390/ijerph120201703>
55. Xie, X., Hao, M., Ding, F., Helman, D., Scheffran, J., Wang, Q., Ge, Q., & Jiang, D. (2022). Exploring the direct and indirect impacts of climate variability on armed conflict in South Asia. *iScience*. <https://doi.org/10.1016/j.isci.2022.105258>
56. Yan, X., Cheng, P., Zhang, Q., Li, X., He, J., Yan, X., Zhao, W., & Wang, L. (2022). Comparisons of climate change characteristics in typical arid regions of the Northern Hemisphere. *Frontiers in Environmental Science*. <https://doi.org/10.3389/fenvs.2022.1033326>
57. Zeng, Y., Jia, L., & Menenti, M. (2023). Changes in vegetation greenness related to climatic and non-climatic factors in the Sudano-Sahelian region. *Regional Environmental Change* <https://doi.org/10.1007/s10113-023-02084-5>
58. Zhao, C., Ma, G., Pan, Y., Ren, S., Gao, Y., & Wu, H. (2024). Accurate vegetation destruction detection using remote sensing imagery based on the three-band difference vegetation index (TBDVI) and dual-temporal detection method. *International Journal of Applied Earth Observation and Geoinformation*, 127:103669. <https://doi.org/10.1016/j.jag.2024.103669>

Commented [J133]: use APA Style